NACA RM L55L22

NACA

RESEARCH MEMORANDUM

EXPERIMENTAL TRANSONIC FLUTTER CHARACTERISTICS OF AN UNTAPERED, 45° SWEPTBACK, ASPECT-RATIO-4 WING

By Charles L. Ruhlin

Langley Aeronautical Laboratory
Langley Field, Va.

NATIONAL ADVISORY COMMITTEE
FOR AERONAUTICS

WASHINGTON

March 26, 1956
Declassified February 10, 1959

1U

NACA RM L55L22

NATIONAL ADVISORY COMMITTEE FOR AERONAUTICS

RESEARCH MEMORANDUM

EXPERIMENTAL TRANSONIC FLUTTER CHARACTERISTICS OF AN UNTAPERED, 45° SWEPTBACK, ASPECT-RATIO-4 WING

By Charles L. Ruhlin

SUMMARY

The flutter characteristics of an untapered, 45° sweptback, aspect-ratio-4 wing were experimentally determined at Mach numbers from 0.85 to 1.34. The results of this investigation were included in NACA RM L55E19a and are repeated herein along with additional information on the models, the tests, and the results of the flutter calculations. A comparison has been made of the present results with those obtained in a previous investigation (NACA RM L55I13a) of a wing having a taper ratio of 0.6 and the same sweep and aspect ratio as the present plan form. This comparison indicated that at subsonic Mach numbers the change in taper ratio had little effect on the flutter-speed ratios (ratios of experimental to calculated flutter speed), whereas at supersonic Mach numbers the untapered wing had lower flutter-speed ratios.

INTRODUCTION

The transonic flutter characteristics of a series of thin, cantilever wings having systematically varied plan forms have been presented in reference 1. Each wing plan form of reference 1 had a taper ratio of 0.6; plan forms having aspect ratios of 4 had sweepback angles of 0°, 30°, 45°, $52\frac{1}{2}$°, and 60°, and plan forms having aspect ratios of 2.4 and 6.4 had sweepback angles of 45°.

In the present flutter investigation, which covered a Mach number range from 0.85 to 1.34, the plan-form variations of reference 1 was extended to a wing having a taper ratio of 1.0, a sweepback angle of 45°, and an aspect ratio of 4. The results of this investigation were included in reference 2, and are repeated herein along with additional information on the models, the tests, and the results of the flutter calculations. A comparison is made herein of the present results with those obtained in reference 1 for a wing having a taper ratio of 0.6 and the same sweep and aspect ratio as the present plan form.

SYMBOLS

a distance, in wing semichords, from midchord to elastic-axis position, measured perpendicular to quarter-chord line; positive for elastic axis behind midchord

A aspect ratio of full-span wing including body intercept, $\frac{(\text{Span})^2}{\text{Area}}$

A_g aspect ratio of exposed panel of semispan wing, $\frac{(\text{Exposed span})^2}{\text{Exposed area}}$

b half-chord of wing measured perpendicular to quarter-chord line, ft

EI bending stiffness, lb-in.^{2}

f_{h_1} first bending natural frequency, cps

f_{h_2} second bending natural frequency, cps

f_t first torsional natural frequency, cps

f_α uncoupled first torsion frequency, cps,

$$\left(f_t \left[1 - \frac{\left(\frac{x_\alpha}{r_\alpha} \right)^2}{1 - \left(\frac{f_{h_1}}{f_t} \right)^2} \right]^{1/2} \right)$$

g_{h_1} structural damping coefficient in first bending mode

GJ torsional stiffness, lb-in.^{2}

I_α mass moment of inertia of wing about elastic axis per unit length, slug-ft^2/ft

l length of wing panel outside of fuselage (exposed wing panel) measured along quarter-chord line, ft

m mass of wing per unit length, slugs/ft

M_e Mach number at flutter

q_e dynamic pressure at flutter, lb/sq ft

r_α nondimensional radius of gyration of wing about elastic axis, $\left(\sqrt{\frac{I_\alpha}{mb^2}}\right)$

V_e experimental flutter speed taken parallel to air stream, ft/sec

V_R reference flutter speed taken parallel to air stream, ft/sec

V_e/V_R nondimensional flutter-speed ratio

x_{cg} distance of center of gravity behind leading edge measured perpendicular to quarter-chord line, percent chord

x_{ea} distance of elastic axis behind leading edge measured perpendicular to quarter-chord line, percent chord

x_α distance, in wing semichords, from wing elastic-axis position to wing center of gravity, measured perpendicular to quarter-chord line; positive for center of gravity behind elastic axis

η nondimensional coordinate along quarter-chord line, fraction of length l

λ taper ratio, $\frac{\text{Chord at tip measured streamwise}}{\text{Chord in plane of symmetry}}$

Λ angle of sweepback of wing quarter-chord line, deg

μ_e wing-mass-density ratio at flutter $\left(\frac{m}{\pi\rho_e b^2}\right)$

ρ_e density of the air at flutter, slugs/cu ft

ω_e angular experimental flutter frequency, radians/sec

ω_R angular reference flutter frequency, radians/sec

ω_α angular uncoupled torsional frequency, radians/sec

MODELS

The wing plan form investigated had a taper ratio of 1.0, 45° of sweepback, and an aspect ratio of 4. The wing had a 65A004 airfoil section measured in a streamwise direction. Three semispan wing models, designated as wings 1, 2, and 3, were used in the tests. A sketch and a photograph of a model wing are shown in figures 1 and 2. The wings were constructed of 2024-T (formerly 24ST) aluminum alloy. In the exposed panel of each wing, a pattern of holes was drilled normal to the chord plane. The holes were filled with a polysulfide rubber compound, the outer surface of which was made flush with the remaining metal. The hole sizes were selected by the use of reference 3 to give a stiffness that would allow the wings to flutter within the dynamic-pressure range of the test facility. Three odd-sized holes located near the midspan (fig. 1) were drilled for use in a later investigation. Strain gages (fig. 2), used to indicate the occurrence of flutter and to measure the flutter frequency, were externally mounted on the top and bottom surfaces near the wing root.

The geometric and measured physical properties of the model wings are presented in tables I and II. The nodal lines associated with the second and third bending and first torsional natural modes of vibration of a typical model wing are shown in figure 3. Shown also in figure 3 is the location of the elastic axis determined with the wing clamped along a line perpendicular to the leading edge and passing through the intersection of the wing trailing edge and root. Though the torsional- and bending-stiffness distributions of the tested wings were not obtained, the results of stiffness measurements of three similarly constructed wings are shown in figure 4.

TEST APPARATUS AND TECHNIQUE

The experimental results were obtained from tests conducted in the Langley transonic blowdown tunnel. The tunnel has a slotted, octagonal test section which measures approximately 26 inches between flats. At any predetermined Mach number up to about 1.45, a stagnation pressure of up to 75 pounds per square inch may be obtained in the test section. This tunnel is particularly useful for flutter investigations in that a constant Mach number may be maintained in the test section while the stagnation pressure, and therefore the air density, is varied. However, it should be noted that the Mach number does not uniquely define the velocity in the test section since during the operation of the tunnel, as air in the reservoir is expended, the stagnation temperature constantly decreases.

Although semispan wings were used exclusively in the present tests, the results of reference 1 indicate that the experimental flutter data obtained with semispan wings are in agreement with those obtained using full-span wings.

For each run (defined as one operation of the tunnel from valve opening to valve closing), the wing was clamped horizontally at 0° angle of attack to a 3-inch-diameter fuselage-sting located along the center line of the tunnel (fig. 1). To avoid the formation of bow shock waves in the tunnel, the sting extended upstream into the subsonic flow region of the tunnel. The sting had a fundamental frequency of about 15 cycles per second.

During each run, the output of the wing strain gages, the test section stagnation temperature, and the test section stagnation and static pressures were continuously recorded by means of a recording oscillograph. Models used in more than one run were checked for structural damage by visual inspection and by comparing natural frequencies of the model obtained before and after each run.

A more complete description of the tunnel, the test procedure, and the instrumentation are given in reference 1.

METHOD OF ANALYSIS

In the presentation of the results each experimental flutter speed has been divided by a calculated or reference flutter speed. The flutter-speed ratio so formed is used in an effort to separate the effects of plan form and Mach number variations from the effects of variations in the other test and model parameters. The method of calculating the reference flutter speed was the same as that used in reference 1 and was based on the method of reference 4. Briefly, the method consists of a Rayleigh type analysis in which two-dimensional, incompressible aerodynamic coefficients are employed and the flutter-mode shape is represented by a superposition of the uncoupled, vibrational-mode shapes of a uniform, cantilever beam. In the present calculations, the first and second bending and first torsional uncoupled mode shapes of a uniform, cantilever beam were used. The natural torsional frequencies were uncoupled for use in the analysis by employment of the formula given in the list of symbols. The natural bending frequencies were used as the uncoupled values.

RESULTS AND DISCUSSION

General Comments

The flutter obtained with the wings of the present investigation was of the bending-torsion type, and the flutter usually occurred with a sudden buildup from random oscillations. However, during two runs, both at supersonic speeds, a period of doubtful flutter characterized by intermittent sinusoidal oscillations of the wing preceded definite flutter. These periods of doubtful flutter are defined (as in ref. 1) as low damping regions.

Presentation of the Results

Results of the present investigation are presented in figure 5 as a plot of the flutter-speed ratio as a function of Mach number. Data from reference 1 are also shown for a plan form having the same sweep angle and aspect ratio as the present wing but having a taper ratio of 0.6. A low damping region is indicated by a dashed line leading to a symbol. The paths of the dashed lines are indicative of the tunnel operating characteristics during the runs.

A compilation of the present experimental and analytical results is given in table III. The table is self-explanatory with the exception of the second and third columns. In the second column, preceding the dash marks are the run numbers; following the dash marks are the numbers which designate the order from the beginning of the run in which each data point occurred. In the third column, the following letter code is used to identify the nature of each data point:

Condition:

The start of a low damping region preceding flutter	D
The start of sustained or definite flutter preceded by a low damping region	S
The start of definite flutter not preceded by a low damping region	C

Discussion

From Mach numbers 0.85 to 1.05 (fig. 5) the flutter-speed ratio of the present wing remained approximately constant at a value of about 1.05. Above a Mach number of 1.05, the flutter-speed ratio increased with Mach number to a value of about 1.44 at a Mach number of 1.34.

Comparison of the data of reference 1 with those of the present investigation (fig. 5) indicates that a change in the taper ratio from 0.6 to 1.0, for a 45° sweptback, aspect-ratio-4 plan form, has very little effect on the flutter-speed ratios at subsonic Mach numbers. At supersonic Mach numbers the increase in taper ratio resulted in decreases in the flutter-speed ratio; the percentage decrease in flutter-speed ratio increased with Mach number to a value of 17 percent at a Mach number of 1.34.

CONCLUSIONS

The results of an investigation of the transonic flutter characteristics of an untapered wing plan form having 45° of sweepback and an aspect ratio of 4 have indicated the following:

1. The flutter-speed ratio remained approximately constant at a value of about 1.05 at Mach numbers from 0.85 to 1.05.

2. Above a Mach number of 1.05, the flutter-speed ratio increased so that the value at a Mach number of 1.34 was approximately 1.44.

3. Comparison of previous results with those of the present investigation indicates that changing the taper ratio from 0.6 to 1.0, for a 45° sweptback, aspect-ratio-4 plan form, results in reductions of the flutter-speed ratios at supersonic Mach numbers; the reduction was about 17 percent at a Mach number of 1.34.

Langley Aeronautical Laboratory,
National Advisory Committee for Aeronautics,
Langley Field, Va., December 1, 1955.

REFERENCES

1. Unangst, John R., and Jones, George W., Jr.: Some Effects of Sweep and Aspect Ratio on the Transonic Flutter Characteristics of a Series of Thin Cantilever Wings Having a Taper Ratio of 0.6. NACA RM L55I13a, 1955.

2. Loftin, Laurence K., Jr.: Flutter Characteristics of Swept Wings at Transonic Speeds. NACA RM L55E19a, 1955.

3. Land, Norman S., and Abbott, Frank T., Jr.: Method of Controlling Stiffness Properties of a Solid-Construction Model Wing. NACA TN 3423, 1955.

4. Barmby, J. G., Cunningham, H. J., and Garrick, I. E.: Study of Effects of Sweep on the Flutter of Cantilever Wings. NACA Rep. 1014, 1951. (Supersedes NACA TN 2121.)

TABLE I.- GEOMETRIC PROPERTIES OF MODELS

NACA section (streamwise)	65A004
A	4
Λ, deg	45
λ	1.0
A_g	1.57
Span, ft	1.166
l, ft	0.648
b, ft	0.103

TABLE II.- PHYSICAL PROPERTIES OF MODELS

Parameter	Wing number		
	1	2	3
x_{ea}, percent chord	42.5	not measured*	not measured*
x_{cg}, percent chord	44.8	--do--	Do.
m, slugs/ft	0.00677	--do--	Do.
x_α	0.05	--do--	Do.
a	-0.15	--do--	Do.
r_α^2	0.25	--do--	Do.
g_{h_1}	0.007	0.008	0.005
f_{h_1}, cps	42.3	41.2	41.7
f_{h_2}, cps	240	241	242
f_t, cps	376	380	375
f_α, cps	374.4	378.4	373.4
$\left(f_{h_1}/f_\alpha\right)^2$	0.0128	0.0119	0.0125
$\left(f_{h_2}/f_\alpha\right)^2$	0.4109	0.4056	0.4200

*The values of the tabulated parameters x_{ea} to r_α^2 inclusive of wings 2 and 3 were assumed in the reference speed calculations to be equal to those of wing 1.

TABLE III.- COMPILATION OF ANALYTICAL AND TEST RESULTS

Wing number	Run-point no.	Flutter point code	M_e	V_e/V_R	ρ_e, slugs/cu ft	μ_e	$\sqrt{\mu_e}$	ω_α, radians/sec	ω_R/ω_α	ω_R, radians/sec	ω_e, radians/sec	ω_e/ω_R	V_e, ft/sec	V_R, ft/sec	$V_e/b\omega_\alpha$	$V_R/b\omega_\alpha$	q_e, lb/sq ft
1	4-1	C	1.319	1.441	0.0041	49.02	7.00	2353	0.392	922.4	1106	1.199	1246.7	865.1	5.142	3.568	3224.2
↓	6-1	C	1.214	1.281	.0032	62.50	7.91	↓	.367	863.6	942	1.091	1194.8	933.0	4.928	3.848	2319.8
	7-1	D	1.027	1.036	.0024	83.33	9.13		.334	785.9	685	.872	1060.7	1024.1	4.375	4.224	1375.2
	7-2	S	1.055	1.064	.0025	81.30	9.02		.337	793.0	741	.934	1081.5	1016.4	4.461	4.192	1461.6
	8-1	C	1.054	1.049	.0025	81.30	9.02		.337	793.0	691	.871	1066.3	1016.4	4.398	4.192	1424.2
	9-1	C	1.022	1.055	.0028	71.43	8.45		.353	830.6	735	.885	1027.0	973.4	4.236	4.015	1497.6
	10-1	C	.970	1.034	.0031	65.79	8.11		.361	849.4	704	.829	980.6	948.0	4.044	3.910	1483.2
	12-1	C	.959	1.060	.0033	60.61	7.79		.369	868.3	735	.846	977.3	921.6	4.031	3.801	1598.4
3	14-1	C	.978	1.077	.0034	60.24	7.76	2346	.372	872.7	729	.835	989.9	918.8	4.095	3.801	1647.4
↓	15-1	C	.911	1.058	.0041	49.50	7.04	↓	.392	919.6	798	.868	915.3	865.2	3.786	3.579	1722.2
	16-1	C	.847	1.053	.0053	38.46	6.20		.414	971.2	854	.879	844.4	801.6	3.493	3.316	1883.5
2	18-1	C	1.340	1.411	.0045	44.84	6.70	2378	.398	946.4	1049	1.108	1198.8	849.8	4.892	3.468	3260.2
↓	22-1	D	1.136	1.096	.0025	82.64	9.09	↓	.335	796.6	741	.930	1129.6	1030.1	4.610	4.204	1566.7
	22-2	S	1.199	1.209	.0032	63.29	7.96		.365	868.0	867	.999	1141.8	944.6	4.660	3.855	2093.8
	23-1	C	1.180	1.219	.0033	62.50	7.91		.366	870.3	898	1.032	1146.8	940.9	4.680	3.840	2141.3

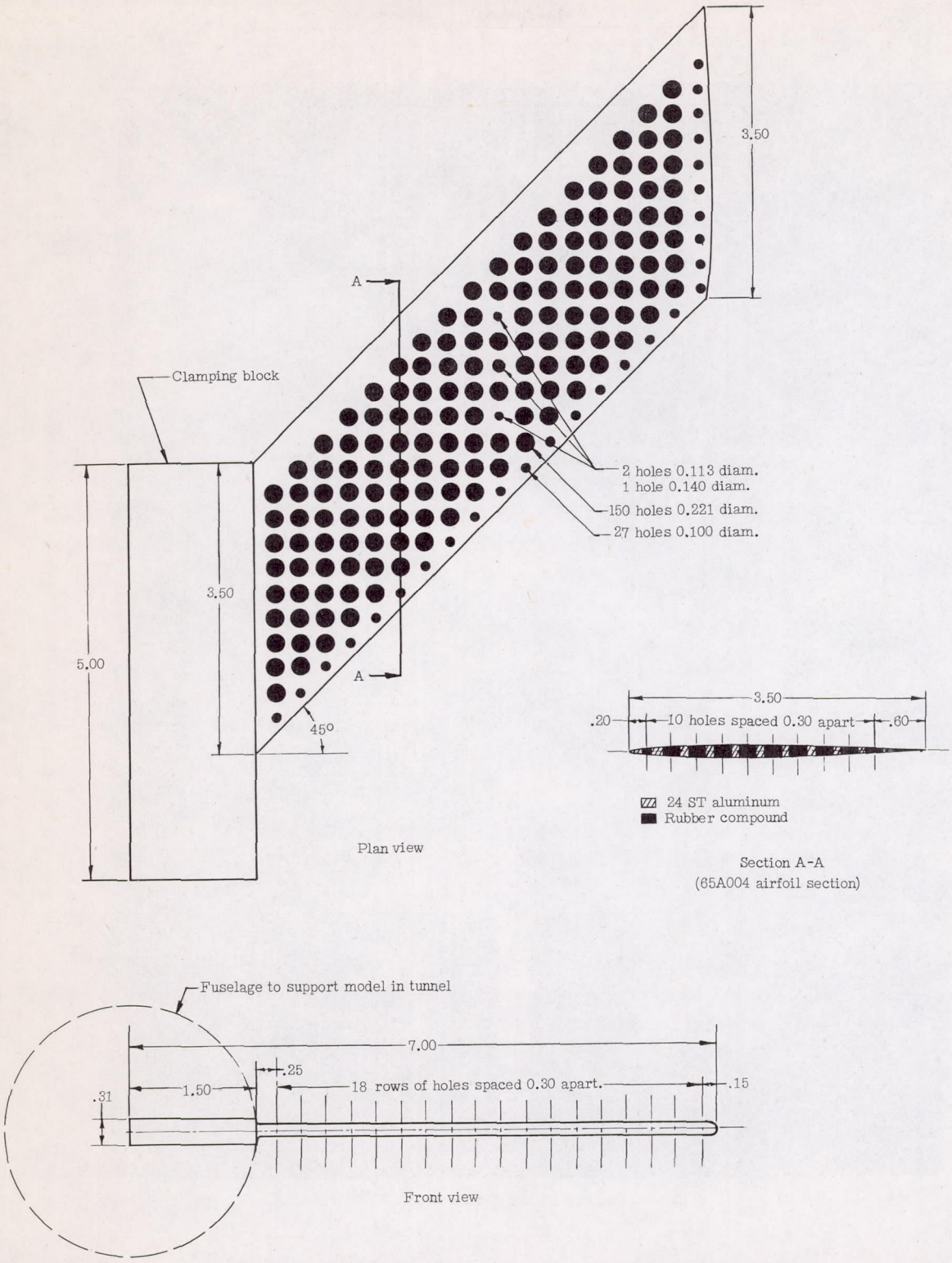


Figure 1.- Sketch of model wing. All dimensions are in inches.

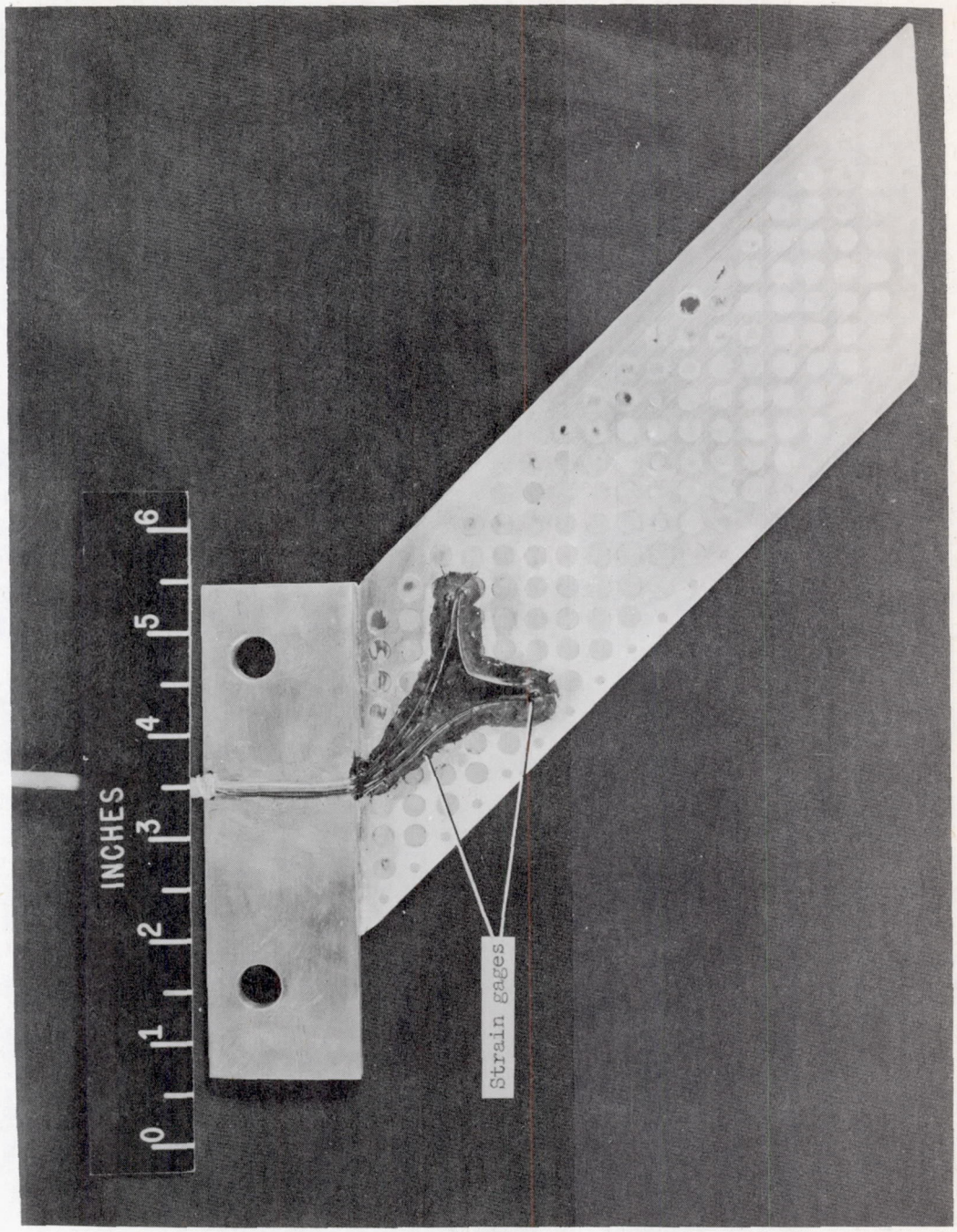


Figure 2.- A photograph of a model wing. L-87869.1

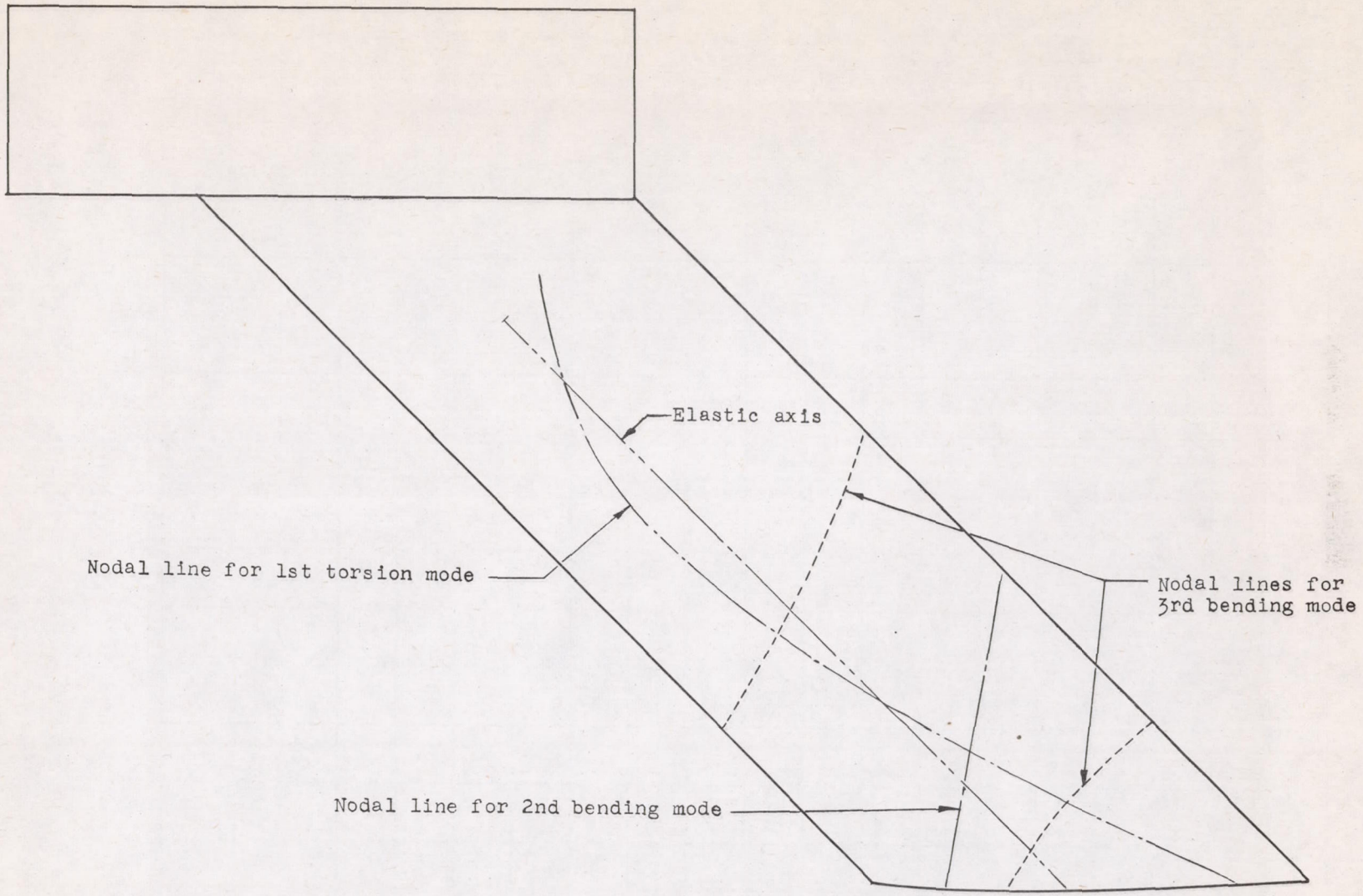


Figure 3.- Nodal lines associated with the natural modes of vibration of a typical model.

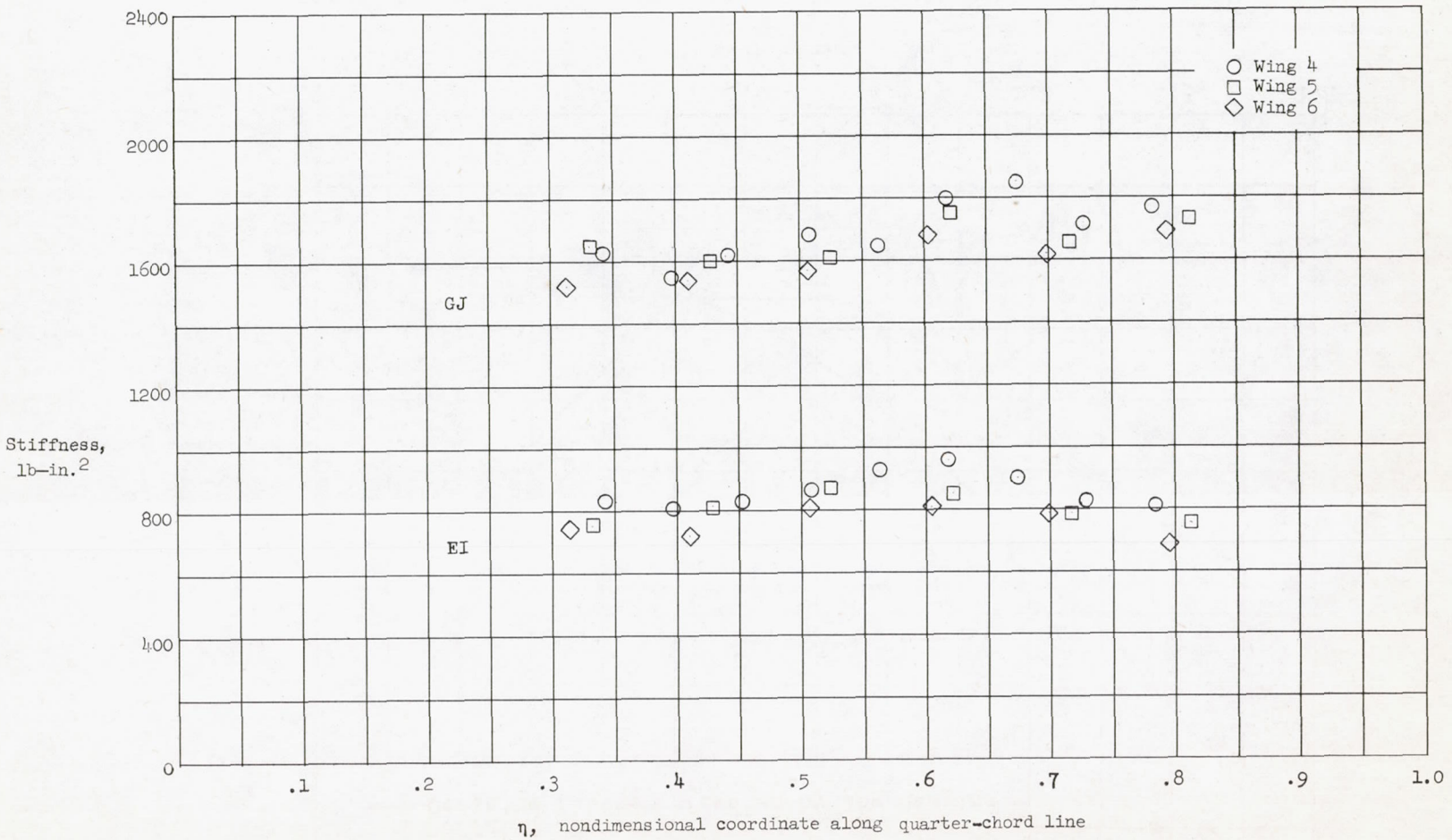


Figure 4.- Measured torsional- and bending-stiffness distribution along the quarter-chord line of three wings similar to the tested models.

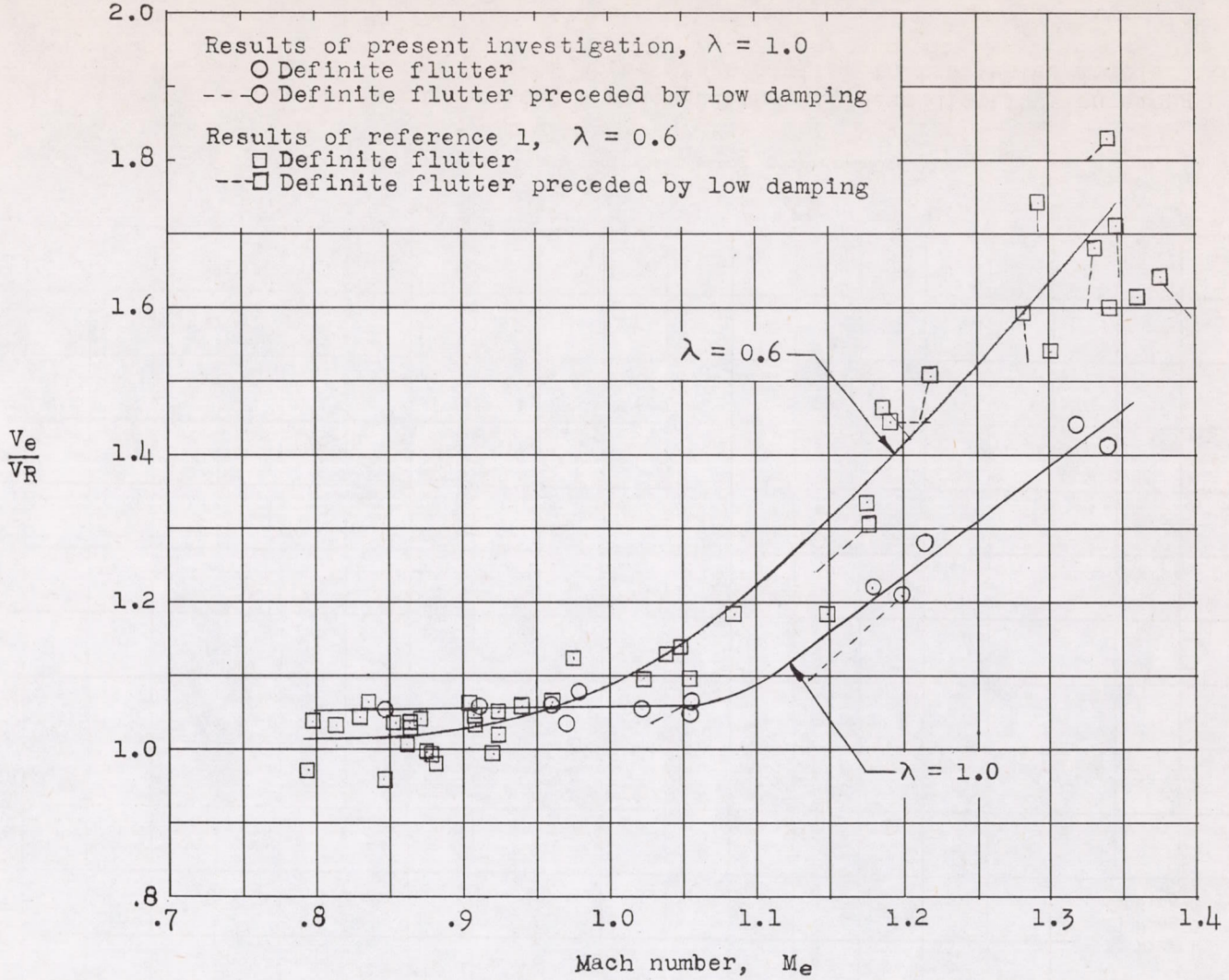


Figure 5.- Mach number effect on flutter-speed ratio of wings having aspect ratio of 4, sweepback of 45°, and taper ratios of 1.0 and 0.6.